Long-distance correlation and zonal flow structures induced by mean $E \times B$ shear flows in the biasing H-mode at TEXTOR

Y. Xu, S. Jachmich, R. R. Weynants, M. Van Schoor, M. Vergote, A. Krämer-Flecken, O. Schmitz, B. Unterberg, C. Hidalgo, and TEXTOR Team

Citation: Physics of Plasmas **16**, 110704 (2009); doi: 10.1063/1.3265367
View online: https://doi.org/10.1063/1.3265367
View Table of Contents: http://aip.scitation.org/toc/php/16/11
Published by the American Institute of Physics

Long-distance correlation and zonal flow structures induced by mean $E \times B$ shear flows in the biasing H-mode at TEXTOR

Y. Xu,[1] S. Jachmich,[1] R. R. Weynants,[1] M. Van Schoor,[1] M. Vergote,[1] A. Krämer-Flecken,[2] O. Schmitz,[2] B. Unterberg,[2] C. Hidalgo,[3] and TEXTOR Team
[1]*Laboratoire de Physique des Plasmas, Laboratorium voor Plasmafysica, Association "Euratom-Belgian State," Ecole Royale Militaire, Koninklijke Militaire School, Trilateral Euregio Cluster, B-1000 Brussels, Belgium*
[2]*Institute für Energieforschung-Plasmaphysik, Forschungszentrum Jülich, Association EURATOM/FZJ, Trilateral Euregio Cluster, D-52425 Jülich, Germany*
[3]*Laboratorio Nacional de Fusion, Association EURATOM-CIEMAT, 28040 Madrid, Spain*

(Received 16 July 2009; accepted 27 October 2009; published online 18 November 2009)

Long-distance toroidal correlations of potential and density fluctuations have been investigated at the TEXTOR tokamak [H. Soltwisch *et al.*, Plasma Phys. Controlled Fusion **26**, 23 (1984)] in edge electrode-biasing experiments. During the biasing-induced H-mode, the *dc* $E \times B$ shear flow triggers a zonal flow structure and hence long-distance correlation in potential fluctuations, whereas for density fluctuations there is nearly no correlation. These results indicate an intimate interaction between the mean and zonal flows, and the significance of long range correlations in improved-confinement regimes. [doi:10.1063/1.3265367]

It is well known that the $E \times B$ shear flows play a crucial role in reducing turbulent transport in magnetically confined plasma, via decorrelating turbulence eddies, and leading consequently to a formation of transport barriers and improvement of plasma confinement.[1,2] Shear decorrelation of turbulence can and has been shown to occur by mean $E \times B$ flows,[3,4] but can also result from time-varying $\tilde{E} \times B$ flows, such as occurring in zonal flows (ZFs) identified as toroidal and poloidal symmetric potential structures ($m=n=0$) with finite radial wavelength.[5] Such ZFs might thus also be important ingredients in regulating turbulence and hence take part in explaining the transition from low to high (L-H) confinement regimes.[6–9] Investigations into ZFs have been intensified recently, both theoretically and experimentally as reviewed in Refs. 10 and 11. They are helpful for confinement as they extract energy from ambient turbulence via nonlinear interaction and in return, quench them by shear decorrelation. Moreover, the ZFs themselves do not drive any radial transport and thus give no free energy for turbulence.

As the ZF has a $n=0$ mode, a cross correlation of fluctuations over a long distance along the B field line is expected. The long-distance correlation (LDC) is therefore an important experimental indicator of the ZFs. Pioneering work on identification of LDC can be found in Refs. 12 and 13. Very recently, in the TJ-II stellarator[14] an amplification of the LDC by biasing electric fields has been found in potential fluctuations during the transition to improved confinement. In the ISTTOK tokamak,[15] the LDC of potential fluctuations displays bursty features and couples with reduced turbulent transport. The results provoke interests of multiscale physics, i.e., interaction between small-scale turbulence and large-scale coherent structures. More recently, in the TJ-K torsatron,[16] a strong increase in the LDC in both potential and density fluctuations was observed due to the biasing-induced shear flow. This result again points out an interaction between mean and zonal flows.

In this investigation, we measured the LDC in the TEXTOR tokamak in biasing H-mode experiments. In this letter, we report the first observation that a ZF structure and the LDC are triggered by *dc* $E \times B$ shear flows during the H-mode phase.

The experiments were performed in Ohmic deuterium discharges in TEXTOR with following parameters: $R=175$ cm, $a \approx 48$ cm, $B_T=2.25$ T, $I_p=200$ kA, and line-averaged densities $\bar{n}_{e0}=(1.0-2.0)\times 10^{19}$ m^{-3}. For measuring the LDC of edge fluctuations along the toroidal direction, two movable Langmuir probe arrays[17] were installed at two approximately opposite locations of the torus (over a distance ~ 7.0 m) in the midplane of the low-field side. Both arrays were operated to detect the floating potential (V_f) and ion saturation current (I_s) and their fluctuations with a sampling rate of 500 kHz. In each discharge, one array is stationary while the other is fast reciprocating. From shot to shot, the radial position of the stationary probe can be altered. In order to achieve an improved-confinement regime and also to explore the possible interplay between the mean $E \times B$ shear flow and the LDC, a biasing voltage was applied between the toroidal belt limiter and a graphite electrode inserted at $r \approx 41$ cm.

Typical discharge waveforms are plotted in Fig. 1. From Figs. 1(a) and 1(c), we can see that the biasing voltage (V_{bia}), ramping from 0 to 300 V and then held constant for 1 s, was applied in the stationary discharge stage. As seen in the shaded zone in Fig. 1(b), during biasing the line-averaged density increases and D_α keeps almost constant, indicating an improvement of particle confinement. Details on the biasing H-mode have been described earlier.[3,4,18] Figure 1(d) shows the time trace of the fast probe, which moves from the scrape-off layer (SOL) into the edge inside the last closed flux surface (LCFS). Meanwhile the stationary probe stays also inside the LCFS (not shown here). For a comparison between the "Ohmic phase" before biasing and the phase during "biasing H-mode," the fast probe plunges twice in one discharge.

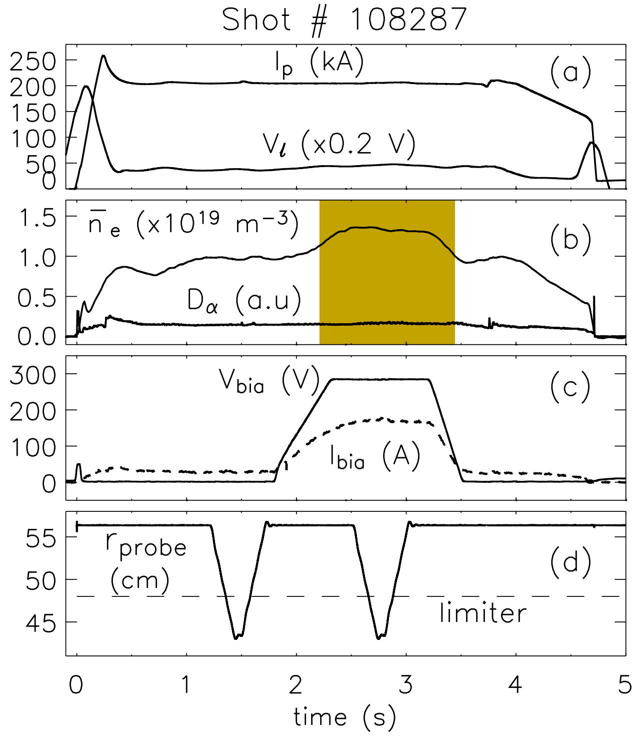

FIG. 1. (Color online) Time evolution of discharge parameters in an edge electrode-biasing H-mode experiment at TEXTOR. (a) Plasma current I_p and loop voltage V_l; (b) line-averaged density and D_α emission on limiter; (c) voltage (solid curve) and current (dashed curve) on electrode; (d) radial position of fast reciprocating probes (dashed line denotes limiter location).

The results of the LDC in V_f and I_s fluctuations between the two probes are illustrated in Fig. 2 for both the Ohmic (before biasing) and biasing H-mode phases. The top panels show similar time traces of the fast probe, moving from the SOL into the edge. For the stationary probe, a schematic is shown for its radial position at r=46.2 cm as a reference probe. The toroidal cross correlation between the signals x and y on the respective probes is defined as $C_{xy}(\tau) = \langle[x(t+\tau)-\bar{x}][y(t)-\bar{y}]\rangle / \sqrt{\langle[x(t)-\bar{x}]^2\rangle\langle[y(t)-\bar{y}]^2\rangle}$, where τ is

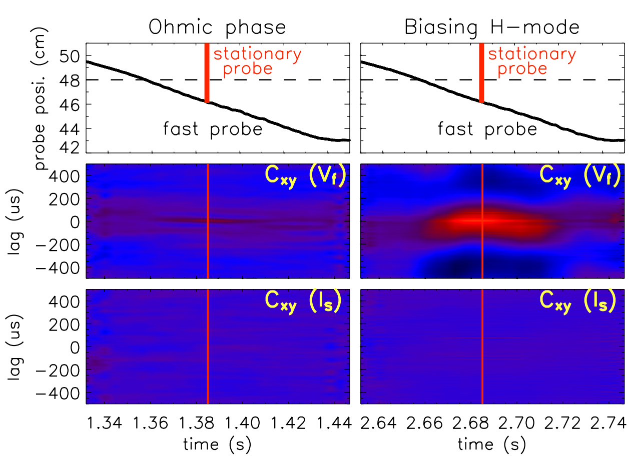

FIG. 2. (Color online) Time history of fast/stationary probes and the contour plot of cross correlation between V_f (middle panels) and I_s (bottom panels) fluctuations measured before (left column) and during (right column) the biasing H-mode (No. 108288). The dashed lines on top panels denote limiter locus. The vertical red lines in contour plots denote the time when the two probes are at the same radial location.

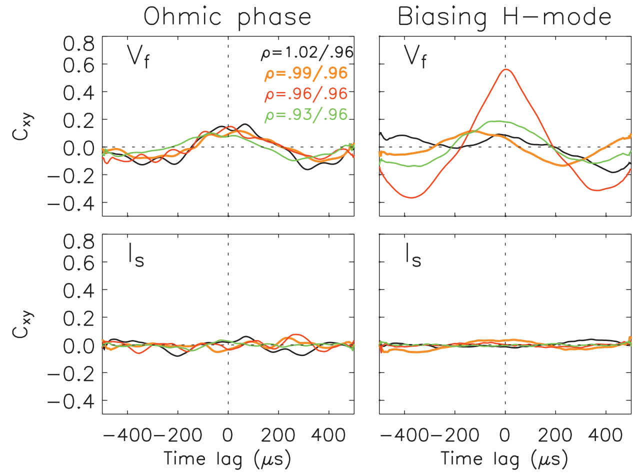

FIG. 3. (Color) Cross-correlation functions for V_f and I_s signals measured by the fast/stationary probe at different radial positions (normalized to a) before (left column) and during (right column) the biasing H-mode.

the time lag. The corresponding time evolutions of the contour plot of $C_{xy}(\tau)$ of V_f and I_s fluctuations are shown in lower panels. Before biasing there is a small C_{xy} in V_f, while during biasing a significant long range correlation appears when the fast probe passed through the radial position of the stationary probe. The LDC covers a radial range of about 3 cm. However, for the I_s signal both before and during biasing there is nearly no correlation. To verify that the LDC is caused by electrostatic modes, the possible impact due to magnetohydrodynamic activities has been excluded by checking magnetic pick-up-coil signals. To view in more details, the $C_{xy}(\tau)$ of V_f and I_s measured at different radial positions (normalized to a) of the fast probe are shown in Fig. 3 by different colors. The fast probe moves from $\rho = r/a = 1.02$ to 0.93 whereas the stationary probe stays at $\rho = 0.96$. The figure shows the following: (i) without biasing the C_{xy} of V_f is larger than I_s although both are small in Ohmic phase; (ii) during biasing the maximum C_{xy} of V_f occurs when the two probes are at the same radial location; (iii) the maximum $C_{xy}(\tau)$ of V_f in H-mode has roughly a zero time lag, implying an in-phase fluctuation of V_f between the two distant probes. In the experiment, the radial position of the stationary probe has been varied from $\rho=0.97$ to 0.94 in different shots. It appears that during biasing the maximum C_{xy} of V_f always takes place at the location where the two probes are around the same flux surface.

Figure 4 plots the frequency spectrum of V_f fluctuations ($\tilde{V}_f$) measured by the two probes at the maximum C_{xy} location. In the Ohmic case, the frequency spectra on both probes are broad and display small coherent modes around 2 and 10 kHz. With biasing, the fluctuation power of V_f at high frequencies (>4 kHz) is generally reduced, in accordance with the paradigm of $E \times B$ shear decorrelation on small-scale turbulence. However, at low frequencies (<3 kHz), there is a strong enhancement of fluctuation power peaked at ~1.6 kHz, coincident with the period (~600 μs) of the maximum C_{xy}. The inset in Fig. 4(b) exhibits the coherence and phase difference in $\tilde{V}_f$ between the two probes in a low frequency range (<5 kHz). At frequencies of 1–2 kHz, the

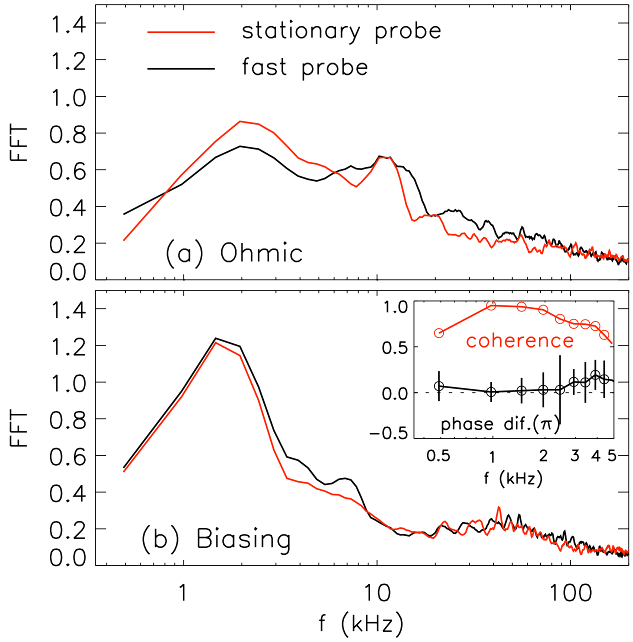

FIG. 4. (Color online) Frequency spectrum of $\tilde{V}_f$ detected by fast/stationary probes at the same flux surface (ρ=0.96) in (a) Ohmic and (b) biasing H-mode phase. The inset in (b) shows the coherence and phase difference (divided by π) between two signals at a low frequency range.

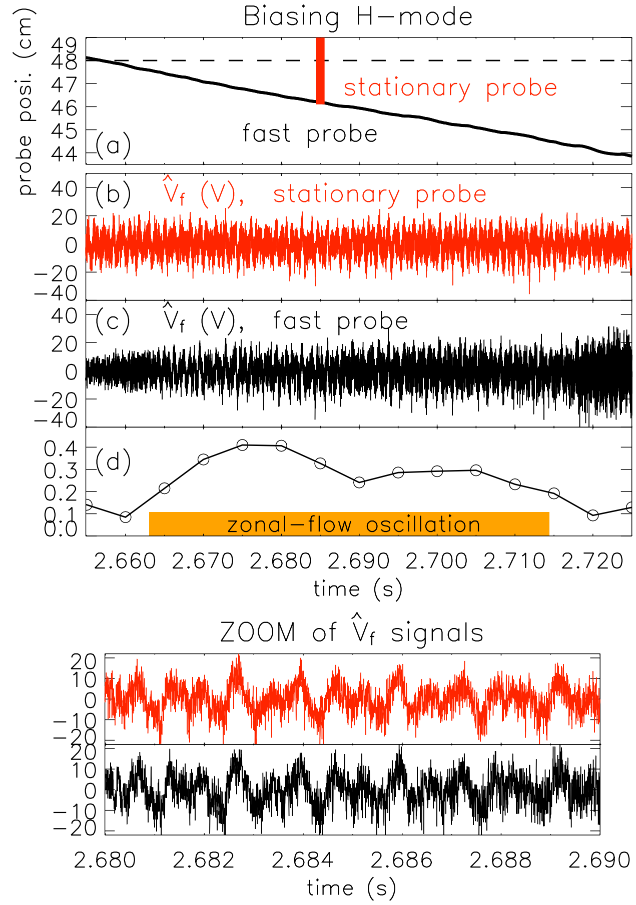

FIG. 5. (Color online) Time evolution of zonal potential oscillations on stationary/fast probe. (a) Probe traces; (b) $\tilde{V}_f$ on stationary probe; (c) $\tilde{V}_f$ on fast probe; (d) the ratio of low frequency ($\leq$4 kHz) to total fluctuation power in $\tilde{V}_f$ signal of the fast probe. The lower zoom panels show low-f oscillations in $\tilde{V}_f$ in a 10 ms time window.

$\tilde{V}_f$ shows very high coherence ($\sim$0.9) and the phase difference is close to zero within the error bars, suggesting a toroidal mode n=0. The results indicate that the LDC is mainly attributed to the low frequency coherent modes.

It should be noted that some of the present results obtained at TEXTOR, such as the amplification of the LDC on V_f during biasing H-mode and no correlation on I_s signals, are similar to those observed in TJ-II stellarator.[14] However, the dominant components in $\tilde{V}_f$ for the LDC show distinct features. In TJ-II the LDC is caused by low frequencies (below 20 kHz) without coherent modes, while in TEXTOR the LDC is dominated by coherent modes ($\sim$1.6 kHz).

To further identify the features of the coherent modes, we look on raw signals of $\tilde{V}_f$ on the two probes, as depicted in Fig. 5. A persistent low frequency oscillation is found on the stationary probe, which appears also on the fast probe in a certain radial range inside the LCFS. To quantify this oscillating feature, we computed the ratio of the fluctuation power at low-f ($\leq$4 kHz) to the total power at different times in the $\tilde{V}_f$ signal of the fast probe. At each time point, the calculation was made by fast Fourier transform with 1024 data points ($\sim$0.48 kHz frequency resolutions). The results are plotted in Fig. 5(d). At time before 2.66 or after 2.72 s, the low-f components take about 10% of the total power, while during that period the fraction increases to 20%–40%. It is interesting to notice that the radial range (44.5–47.5 cm), where the low-f oscillations are present, is exactly located within the mean $E\times B$ flow shear layer induced by the biasing [see Fig. 6(a)]. This fact reveals that the low-f coherent structure is closely related to the mean $E\times B$ flow in the biasing H-mode. The zooms of $\tilde{V}_f$ show slow in-phase oscillations ($f\approx$1.6 kHz) between the two probes, verifying n=0 mode structure. Similar in-phase oscillations in $\tilde{V}_f$ are also seen in poloidally spaced probe pins over a distance of 6.4 mm, in agreement with a poloidally symmetric structure of ZFs. Thus, the observed low-f potential oscillation inside the $E\times B$ shear layer is a ZF structure. In TJ-K torsatron similar ZF-like modes in $\tilde{V}_f$ are also excited by mean $E\times B$ flows.[16] Note that although a mean shear flow is imposed first in the present "active" biasing experiment the presence of H-mode and the LDC (ZF) is almost concurrent. Since ZFs also happen in H-mode without biasing,[19,20] it remains unclear whether the mean flow shear directly excites the ZFs or it triggers the H-mode which then excites the ZFs.

Hitherto two main branches of ZFs have been identified, i.e., finite-frequency geodesic acoustic modes (GAMs) and the zero-mean-frequency (or residual) ZF.[10,11] Comparing the frequency spectra of the ZF in our case with those of residual ZFs or finite-frequency ZFs seen in other machines,[11,13,19,20] it seems that the ZF structure observed by us is similar to the residual ZFs. In addition, we have calculated the autobispectrum of potential fluctuations using techniques introduced in Ref. 21. The results show an increase in the bicoherence in low frequencies ($f<3$ kHz) during the biasing H-mode, in agreement with ZF generation by nonlinear interactions of turbulence.[10]

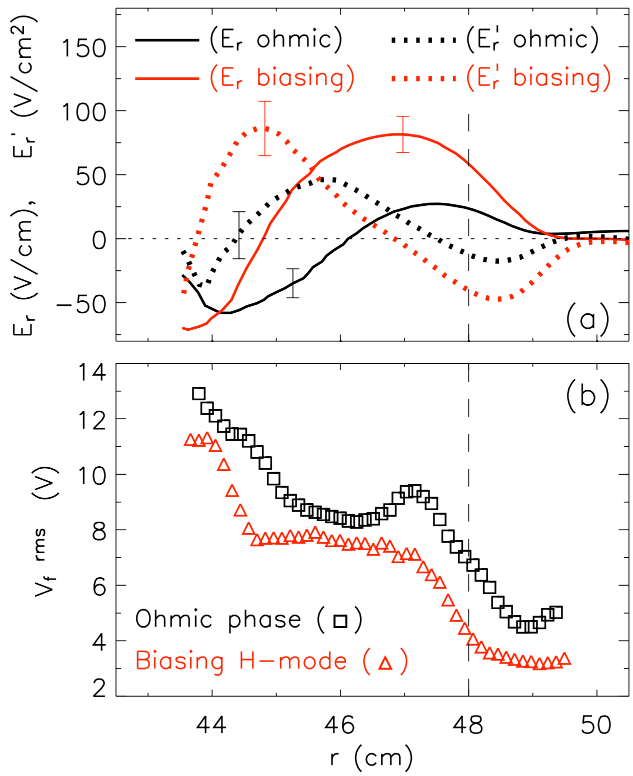

FIG. 6. (Color online) Radial profiles of (a) E_r and E_r shear (E_r') and (b) the rms levels of $\tilde{V}_f$ before (Ohmic) and during the biasing H-mode. The vertical dashed line denotes limiter position.

Since the ZFs are helpful in regulating turbulence, it is appropriate to estimate their contribution by calculating the fluctuating $\tilde{E}\times B$ flow shear rate, and compare it with that of the mean $E\times B$ flow shear driven by biasing. To illustrate these issues, the radial dependencies of the *dc* radial electric field E_r and E_r shear (E_r') before and during biasing H-mode are plotted in Fig. 6 together with root mean square (rms) levels of $\tilde{V}_f$. The $E_r(E_r')$ profile is estimated from the first (second) radial derivative of the plasma potential ($V_f+2.8T_e$), where the electron temperature T_e is measured by a triple-probe model.[22] In the Ohmic phase a naturally occurring E_r shear layer causes a local reduction of fluctuation level around r=46 cm. During biasing H-mode, a large *dc* $E_r\times B$ shear layer is developed. In the same region, a ZF structure with fluctuating $\tilde{E}_r\times B$ shear flows is triggered. The maximum *dc* $E_r\times B$ shear rate ($\omega_{dc}=E_r'/B$) at r=44.7 and 48.5 cm are about 4×10^5 and -3×10^5 s^{-1}, respectively. The ZF structure decays in a radial length of $d_r\approx1$ cm (see Fig. 2). The fluctuating V_f amplitude, $|\tilde{V}_f|$, of the ZF is about 12 V (see Fig. 5). Thus, the fluctuating $\tilde{E}_r\times B$ shear rate due to the ZF is estimated by $\omega_{ZF}=|\tilde{V}_f|/d_r^2B\approx1\times10^5$ s^{-1}. As the ZF shear is varying in time, the resulting actual value of the shear rate is lower than given by the above value. Applying Ref. 23, we found however that in our case the reduction is negligible. The ω_{ZF} is smaller than but comparable with ω_{dc}. Its contribution to the turbulence self-regulation might be significant. In Fig. 6(b), we see an overall reduction of the fluctuation level of $\tilde{V}_f$ from the Ohmic to H-mode phases. At the maximum ω_{dc} locations (r=44.7 and 48.5 cm), the fluctuation reduction is the largest because of stronger ω_{dc}, while in between where ω_{dc} becomes weak the ω_{ZF} could play the major role in the fluctuation reduction. As $\omega_{ZF}<\omega_{dc}$, the decrease is relatively smaller here than on both sides.

In the biasing H-mode, the confinement improvement is accompanied with the generation of edge transport barrier, which is attributed to flow shear suppression on turbulent transport. In addition to mean flows, the presence of the ZFs (LDC) is certainly a positive sign in regulating turbulence and thus helpful in reaching H-mode. Similar ZFs have also been seen in spontaneous H-mode.[6–9,19,20] Our results appear thus to support the significance of ZFs and LDC in improved-confinement regimes.

In conclusion, long range correlations of edge fluctuations have been studied at TEXTOR tokamak in edge biasing experiments. The results show evidence that a *dc* $E\times B$ flow shear triggers a ZF structure and long range correlations in potential fluctuations in the H-mode phase. The time-varying $\tilde{E}\times B$ flows related to this zonal structure could amplify and complement the fluctuation suppression linked to the *dc* $E\times B$ flow shear. Consequently, the ZFs could also play a role in triggering the *L-H* transition. These findings support the critical role of multiscale physics in the *L-H* transition process.

The authors thank Mr. M. Vervier and V. Lancellotti for maintenance of electronic systems of probe measurements, and Dr. M. Lehnen and Professor U. Samm for support of this work.

[1] K. H. Burrell, Phys. Plasmas **4**, 1499 (1997).
[2] H. Biglari, P. H. Diamond, and P. W. Terry, Phys. Fluids B **2**, 1 (1990).
[3] S. Jachmich, G. Van Oost, R. R. Weynants, and J. A. Boedo, Plasma Phys. Controlled Fusion **40**, 1105 (1998).
[4] J. Boedo, D. Gray, S. Jachmich *et al.*, Nucl. Fusion **40**, 1397 (2000).
[5] A. Hasegawa, C. G. Maclennan, and Y. Kodama, Phys. Fluids **22**, 2122 (1979).
[6] P. H. Diamond, M. N. Rosenbluth, E. Sanchez *et al.*, Phys. Rev. Lett. **84**, 4842 (2000); E. Kim and P. H. Diamond, *ibid.* **90**, 185006 (2003).
[7] R. A. Moyer, G. R. Tynan, C. Holland, and M. J. Burin, Phys. Rev. Lett. **87**, 135001 (2001); G. R. Tynan, R. A. Moyer, M. J. Burin, and C. Holland, Phys. Plasmas **8**, 2691 (2001).
[8] H. Punzmann and M. G. Shats, Phys. Rev. Lett. **93**, 125003 (2004).
[9] A. E. White, S. J. Zweben, M. J. Burin, and T. A. Carter, Phys. Plasmas **13**, 072301 (2006).
[10] P. H. Diamond, S.-I. Itoh, K. Itoh, and T. S. Hahm, Plasma Phys. Controlled Fusion **47**, R35 (2005).
[11] A. Fujisawa, Nucl. Fusion **49**, 013001 (2009).
[12] G. R. Mckee, R. J. Fonck, M. Jakubowski *et al.*, Phys. Plasmas **10**, 1712 (2003).
[13] A. Fujisawa, K. Itoh, H. Iguchi *et al.*, Phys. Rev. Lett. **93**, 165002 (2004).
[14] M. A. Pedrosa, C. Silva, C. Hidalgo *et al.*, Phys. Rev. Lett. **100**, 215003 (2008).
[15] C. Silva, C. Hidalgo, H. Figueiredo *et al.*, Phys. Plasmas **15**, 120703 (2008).
[16] P. Manz, M. Ramisch, and U. Stroth, Phys. Plasmas **16**, 042309 (2009).
[17] Y. Xu, M. Van Schoor, R. R. Weynants *et al.*, Nucl. Fusion **47**, 1696 (2007).
[18] R. R. Weynants, G. van Oost, G. Bertschinger *et al.*, Nucl. Fusion **32**, 837 (1992).
[19] G. McKee, 49th Annual Meeting of the APS DPP, 2007, Paper No. YI1.00004.
[20] M. Shats and W. Solomon, New J. Phys. **4**, 30 (2002).
[21] Y. Kim and E. Powers, IEEE Trans. Plasma Sci. **7**, 120 (1979).
[22] S. Chen and T. Sekiguchi, J. Appl. Phys. **36**, 2363 (1965).
[23] T. S. Hahm, M. A. Beer, Z. Lin *et al.*, Phys. Plasmas **6**, 922 (1999).